

Novel Kinetic Model for Heterogeneous Catalysis Based on Free Energy Dissipation via Intermediates Deduced by the Frequency Response Method

Yusuke Yasuda* and Yasuhiro Kuno

Faculty of Science, Toyama University, Toyama 930, Japan

Received: January 7, 1998

A novel kinetic model for heterogeneous catalysis based on the flow of free energy (instead of ordinary mass-flow) is proposed; the chemical kinetic model is valid to interpret a “reaction-rate spectrum” obtainable by a frequency response (FR) technique. The characteristic function to analyze the spectrum derived from the kinetic differential equations contains complex rate constants, $(k + i\omega l)$'s; k denotes the ordinary rate constant at an elementary step, l is the novel rate constant due to the free energy dissipation, and ω is the angular frequency scanned in the FR technique. The conclusion has been confirmed by actual data obtained in a catalytic hydrogenation of propene over Pt and/or Rh metals on the basis of a three-stage model: $X(g) \rightleftharpoons A_X(a) \rightleftharpoons B_X(a) \rightarrow \text{Product}(s)$, where $X(g)$ represents propene or hydrogen molecules in the gas phase; $A_X(a)$ and $B_X(a)$ are the intermediates on the catalysts. This model contains five k 's for the three direct and two reverse reactions and two l 's of A_X and B_X for their two direct reactions. On the basis of the present results, a generic procedure to analyze a reaction-rate spectrum is proposed.

1. Introduction

A “rate spectrum” characteristic of a gas/surface dynamic phenomenon can be obtained by a frequency response (FR) method.¹ Analogous to a spectroscopic method, the FR method seems to be powerful enough to investigate separately various rate processes occurring simultaneously under reactive as well as nonreactive conditions. Although the spectrum of a nonreactive system has been interpreted well by the characteristic function derived from a theoretical rate equation such as Langmuir kinetics,¹ in the case of a reactive system any traditional kinetic equations were not valid and a working hypothesis was needed.²

The aim of this article is to show that the characteristic function to analyze the reaction-rate spectrum can be derived without a hypothesis from a novel kinetic model based on the flow of free energy (instead of the mass-flow) during a reaction; for example, the three-stage model adopted in this work is demonstrated in Figure 1, where w_A and w_B indicate the molar free energy dissipation.

It is a fundamental principle of thermodynamics that the Gibbs free energy of a system, G , always decreases during a reaction under constant pressure and temperature. Nevertheless, the dissipation of G ,

$$dG/dt = d(H - TS)/dt \quad (1)$$

has scarcely been considered, because heat measurements correspond to only the part of dH/dt . Evidently, the rate of a reaction would be dominated by not dH/dt but dG/dt .

2. Theoretical Section

2.1. FR Method. In the present FR method, the gas space V of a gas/surface system reacting at a steady state is perturbed sinusoidally (complex notation will be used):

$$V(t) = \bar{V}\{1 - v \exp(i\omega t)\} \quad (2)$$

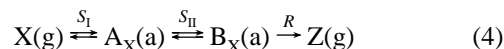
where \bar{V} denotes the mean value of the volume, v (usually ca. 10^{-2}) is the relative amplitude, and ω is the angular frequency of the sinusoidal variation. The pressure variation $P_X(t)$ of a component X perturbed by the volume variation may be expressed in general by

$$P_X(t) = \bar{P}_X\{1 + p_X \exp(i\omega t + \phi_X)\} \quad (3)$$

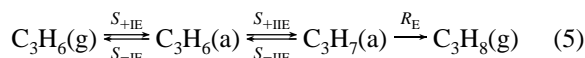
where \bar{P}_X denotes the pressure at the steady state, p_X is the relative amplitude, and ϕ_X is the phase difference between the volume and pressure variations. Since dependence of p_X and ϕ_X on ω are characteristic of the dynamical system, it may be named the “rate spectrum”.

The problem is how to analyze the spectrum and derive rate constants involved in the system.

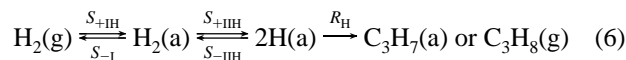
2.2. Three-Stage Model. The following three-stage model for a heterogeneous catalytic reaction is considered in this work:



where $X(g)$ and $Z(g)$ denote gaseous molecules and $A_X(a)$ and $B_X(a)$ are intermediate products; S 's and R denote the overall reaction rates at the elementary steps. For example, in a catalytic hydrogenation of propene, both reactants have been found to follow each three-stage reaction mechanism:^{2,3}



and



where $C_3H_7(a)$ denotes the half-hydrogenated intermediate; the direct and reverse reaction rates are indicated individually.

* Author to whom correspondence should be addressed. E-mail: yasuda@sci.toyama-u.ac.jp. Fax: +81 764 45 6549.

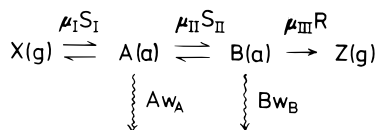


Figure 1. Kinetic model for a heterogeneous catalytic reaction based on the flow of free energy; the free energy dissipations via the intermediate products, A_X and B_X , are represented by $A w_A$ and $B w_B$.

2.3. Basic Equations. Let us consider the flow of free energy by the three-stage model demonstrated in Figure 1 and introduce the molar free energy dissipation w_A and w_B via A_X and B_X , respectively; the unit is [J/min] or [W]. Free energy balances with respect to the two intermediates in the model may be described by

$$A w_A = (\mu_X - \mu_A)(S_{+I} - S_{-I}) - (\mu_A - \mu_B)(S_{+II} - S_{-II}) \quad (7)$$

and

$$B w_B = (\mu_A - \mu_B)(S_{+II} - S_{-II}) - (\mu_B - \mu_Z)R \quad (8)$$

where μ denotes the chemical potential of each component; the subscript E or H is omitted for simplicity. According to the second law of thermodynamics, free energy of a system always dissipates in the course of a reaction, and therefore eqs 7 and 8 may be regarded as basic equations.

2.4. At a Steady State. If the reaction proceeds at a steady state (or $\omega = 0$), considering the reaction mechanism of eq 5 or 6, we have

$$\bar{S}_{+I} - \bar{S}_{-I} = \bar{S}_{+II} - \bar{S}_{-II} = \bar{R} \quad (9)$$

The bar on each letter indicates the rate at the steady state. Substituting eq 9 into eqs 7 and 8, we have

$$\bar{A w}_A = (\mu_I - \mu_{II})\bar{R} \quad (10)$$

and

$$\bar{B w}_B = (\mu_{II} - \mu_{III})\bar{R} \quad (11)$$

where the short notation

$$\mu_I \equiv \mu_X - \mu_A; \quad \mu_{II} \equiv \mu_A - \mu_B; \quad \mu_{III} \equiv \mu_B - \mu_Z \quad (12)$$

for the difference at each stage has been introduced.

2.5. Under Periodic Perturbation. When the pressure of a reactant X is varied in such a way expressed in eq 3, every variable in Figure 1 (i.e., S_I , A , w_A , S_{II} , B , w_B , and R) would also be varied. The basic equations of eqs 7 and 8 lead to

$$\Delta(A w_A) = \mu_I(\Delta S_{+I} - \Delta S_{-I}) - \mu_{II}(\Delta S_{+II} - \Delta S_{-II}) \quad (13)$$

and

$$\Delta(B w_B) = \mu_{II}(\Delta S_{+II} - \Delta S_{-II}) - \mu_{III}\Delta R \quad (14)$$

where Δ means the variation induced by the volume variation of eq 2.

On the other hand, material balances with respect to A and B intermediates lead to

$$(\Delta S_{+I} - \Delta S_{-I}) - (\Delta S_{+II} - \Delta S_{-II}) = \Delta \dot{A} \quad (15)$$

and

$$(\Delta S_{+II} - \Delta S_{-II}) - \Delta R = \Delta \dot{B} \quad (16)$$

where the dot means the time derivative: $\dot{A} \equiv dA/dt$ and $\dot{B} \equiv dB/dt$. Substituting eqs 15 and 16 into eqs 13 and 14, we have

$$\bar{A}\Delta w_A = \mu_I\Delta \dot{A} + (\mu_I - \mu_{II})\{\Delta S_{+II} - \Delta S_{-II} - (\bar{R}/\bar{A})\Delta A\} \quad (17)$$

and

$$\bar{B}\Delta w_B = \mu_{II}\Delta \dot{B} + (\mu_{II} - \mu_{III})\{\Delta R - (\bar{R}/\bar{B})\Delta B\} \quad (18)$$

where the results for \bar{w}_A and \bar{w}_B in eqs 10 and 11 have been substituted. Since Δw_A (or Δw_B) is affected by $\Delta \dot{A}$ (or $\Delta \dot{B}$) as given in eq 17 (and 18), the complementary terms of $\mu_{II}\Delta S_{+II}$ (or $\mu_{III}\Delta R$) in Figure 1 would also be affected by $\Delta \dot{A}$ (or $\Delta \dot{B}$).

Consequently, the variation of ΔS 's and ΔR in eqs 13–16 may be given by (after Taylor series expansion to the first order because of the small perturbation of v in eq 2)

$$\Delta S_{+I}(P_X, A_X) = (\partial S_{+I}/\partial P_X)\Delta P_X \equiv K_{PX}\Delta P_X \quad (19)$$

$$\Delta S_{-I}(P_X, A_X) = (\partial S_{-I}/\partial A_X)\Delta A_X \equiv k_{-AX}\Delta A_X \quad (20)$$

$$\begin{aligned}
 \Delta S_{+II}(A_X, \dot{A}_X; B_X) &= (\partial S_{+II}/\partial A_X)\Delta A_X + (\partial S_{+II}/\partial \dot{A}_X)\Delta \dot{A}_X \\
 &\equiv k_{AX}\Delta A_X + l_{AX}\Delta \dot{A}_X \quad (21)
 \end{aligned}$$

$$\Delta S_{-II}(A_X, B_X) = (\partial S_{-II}/\partial B_X)\Delta B_X \equiv k_{-BX}\Delta B_X \quad (22)$$

$$\begin{aligned}
 \Delta R(B_X, \dot{B}_X) &= (\partial R/\partial B_X)\Delta B_X + (\partial R/\partial \dot{B}_X)\Delta \dot{B}_X \\
 &\equiv k_{BX}\Delta B_X + l_{BX}\Delta \dot{B}_X \quad (23)
 \end{aligned}$$

Here various rate constants (more strictly, “coefficients”) have been introduced. It is noted that only K_{PX} depends on the amounts of catalysts and the others are independent of them; therefore all k 's and l 's may be compared with other data obtained with other catalysts or by other investigators. In consideration of the relations that are valid for harmonic oscillations,

$$\Delta \dot{A} = i\omega\Delta A \quad \text{and} \quad \Delta \dot{B} = i\omega\Delta B \quad (24)$$

it is convenient to introduce the complex rate constants in eqs 21 and 23 defined as

$$k_{AX}^* \equiv k_{AX} + i\omega l_{AX} \quad (25)$$

and

$$k_{BX}^* \equiv k_{BX} + i\omega l_{BX} \quad (26)$$

Substituting eqs 19–23 into eqs 17 and 18, we have [Appendix]

$$\bar{A}\Delta w_A = \{\mu_I + l_A(\mu_I - \mu_{II})\}\Delta \dot{A} \quad (27)$$

and

$$\bar{B}\Delta w_B = \{\mu_{II} + l_B(\mu_{II} - \mu_{III})\}\Delta \dot{B} \quad (28)$$

It is worth noting that both Δw_A and Δw_B are asymptotic to zero as $\omega \rightarrow 0$, and therefore they disappear in ordinary experiments without the forced oscillation. Further it is noted that since every potential difference μ_I , μ_{II} , or μ_{III} vanishes at an equilibrium or in a nonreactive system, eqs 7 and 8 lead to $w_A = w_B = 0$.

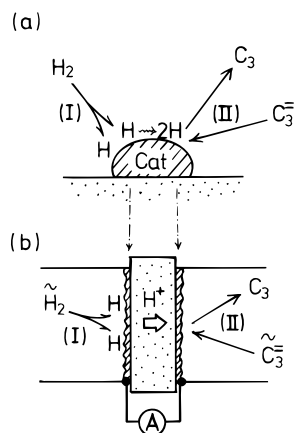


Figure 2. (a) In a usual reactor, a mixture of the two reactants, H₂ and propene (C₃H₆), is contacted with catalysts and the two rate processes, the dissociation (I) and association (II) of H₂ producing propane (C₃H₈), occur simultaneously. (b) The two rate processes, (I) and (II), are separated by a proton-conducting membrane. The migration of atomic hydrogen on catalysts could be detected by current due to the flow of H⁺ across the membrane.

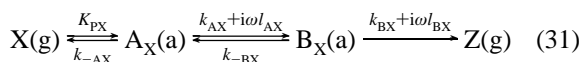
Dividing eq 27 by eq 10 or eq 28 by eq 11, we have

$$\Delta w_A/\bar{w}_A = \{\mu_I/(\mu_I - \mu_{II}) + l_A\}(\Delta\dot{A}/\bar{R}) \quad (29)$$

and

$$\Delta w_B/\bar{w}_B = \{\mu_{II}/(\mu_{II} - \mu_{III}) + l_B\}(\Delta\dot{B}/\bar{R}) \quad (30)$$

2.6. Complex Rate Constants. Consequently, the three-stage model of eq 4 may be characterized by seven rate constants, one *K*, four *k*'s, and two *l*'s:



According to a standard procedure based on material balances, we can easily derive the following two simultaneous equations with respect to the two intermediates:

$$\Delta\dot{A}_X = (K_{PX}\Delta P_X - k_{-AX}\Delta A_X) - (k_{AX}^*\Delta A_X - k_{-BX}\Delta B_X) \quad (32)$$

and

$$\Delta\dot{B}_X = (k_{AX}^*\Delta A_X - k_{-BX}\Delta B_X) - k_{BX}^*\Delta B_X \quad (33)$$

where the complex rate constants in eqs 25 and 26 have been employed.

Substituting eqs 24 into eqs 32 and 33, we can easily solve these simultaneous equations. The final results are

$$\Delta A_X(t) = \{K_{PX}(k_{-BX} + k_{BX}^* + i\omega)/\Phi_X\}\Delta P_X(t) \quad (34)$$

and

$$\Delta B_X(t) = \{K_{PX}k_{AX}^*/\Phi_X\}\Delta P_X(t) \quad (35)$$

where the following abbreviation is introduced:

$$\Phi_X \equiv (k_{-AX} + k_{AX}^* + i\omega)(k_{-BX} + k_{BX}^* + i\omega) - k_{AX}^*k_{-BX} \quad (36)$$

3. Application to Actual Data

3.1. Reaction-Rate Spectra. In a usual reactor shown in Figure 2a, both reactants, H₂ and propene (C₃H₆), are contacted

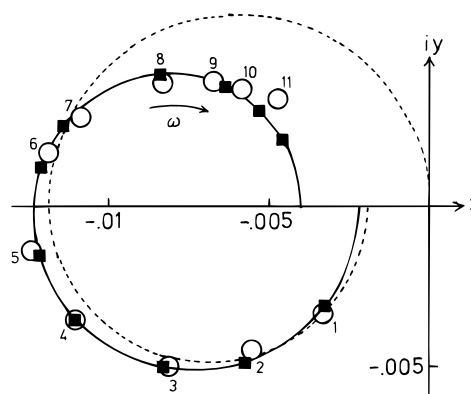


Figure 3. FR data on $\Delta I_E(t)/\Delta P_E(t)$ [mA/Torr] of a H₂(20Torr)/Pt/Rh/C₃H₆(20Torr) system: (○) actual data; (■) simulated results by $J_X^*(\omega)$, of which parameters are given in Table 1. The number corresponds to the angular frequency ω /radians min⁻¹: 1 ($\omega = 0.81$), 2 (=1.70), 3 (=2.69), 4 (=4.68), 5 (=7.24), 6 (=12.9), 7 (=17.4), 8 (=34.7), 9 (=55.0), 10 (=81.3), 11 (=126). The dotted curve represents the most fitted one by $K_C^*(\omega)$.

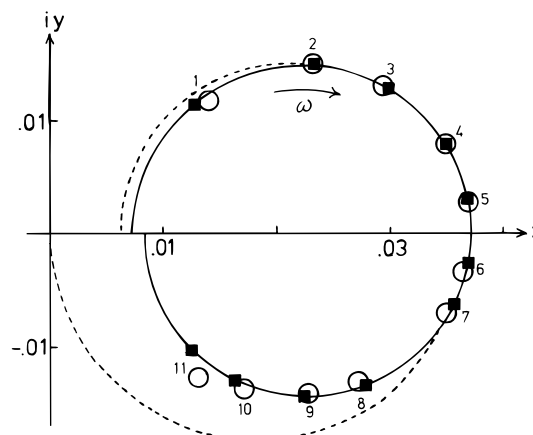


Figure 4. FR data on $\Delta I_H(t)/\Delta P_H(t)$ [mA/Torr] of a H₂(20Torr)/Pt/Rh/C₃H₆(20Torr) system: (○) actual data; (■) simulated results by $J_X^*(\omega)$, of which parameters are given in Table 1. The number corresponds to the angular frequency/radians min⁻¹: 1 (= 0.79), 2 (=1.78), 3 (=2.75), 4 (=4.68), 5 (=7.41), 6 (=12.9), 7 (=18.2), 8 (=40.7), 9 (=58.9), 10 (=91.2), 11 (=135). The dotted curve represents the most fitted one by $K_H^*(\omega)$.

with catalysts so that the dissociation of H₂, (I), and association of 2H to C₃H₆, (II), occur simultaneously. However, in a cell reactor composed of a proton-conducting membrane shown in Figure 2b, the two rate process (I) and (II) are separated and may be investigated distinctly. The reaction-rate spectrum of Figure 2b would become simpler than that of Figure 2a, and therefore more accurate examination for the theoretical expectations proposed in section 2 would be possible.

The apparatus and procedure have been described elsewhere;² pressure of either propene, *P_E*, or hydrogen, *P_H*, was varied sinusoidally and the FR of the system was observed by current *I* due to the flow of H⁺. Typical FR data obtained by different systems with different metals, (i) H₂/Pt/Rh/C₃H₆ and (ii) H₂/Rh/Rh/C₃H₆, are represented in Figures 3–6. Here the short notation H₂/Pt/Rh/C₃H₆, for example, means that H₂ and C₃H₆ are separated by the membrane on both sides of which Pt and Rh metals are deposited.

3.2. Spectrum Analysis. When *P_E* is perturbed, the amounts of H⁺(a) would be affected via the second and third steps of eq 5; the variation in the flow of H⁺ across the membrane may be expressed in this case as

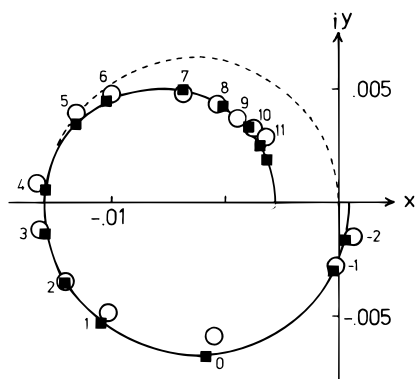


Figure 5. FR data on $\Delta I_E(t)/\Delta P_E(t)$ [mA/Torr] of a $\text{H}_2(20\text{Torr})/\text{Rh}/\text{Rh}/\text{C}_3^{2-}(20\text{Torr})$ system: (○) actual data; (■) simulated results by $J_X^*(\omega)$, of which parameters are given in Table 2. The number corresponds to the angular frequency $\omega/\text{radians min}^{-1}$: -2 ($\omega = 0.12$), -1 (=0.22), 0 (=0.89), 1 (=1.82), 2 (=2.75), 3 (=4.47), 4 (=7.24), 5 (=14.8), 6 (=20.4), 7 (=38.9), 8 (=57.5), 9 (=85.1), 10 (=117.5), 11 (=158). The dotted curve represents the most fitted one by $K_C^*(\omega)$.

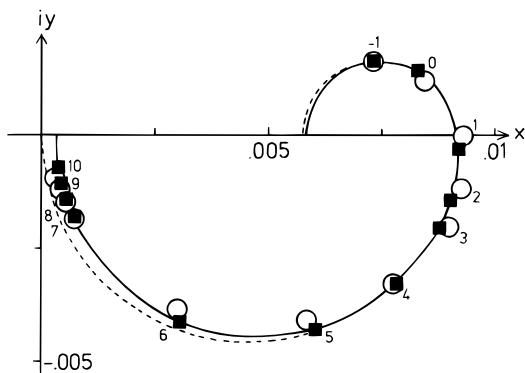
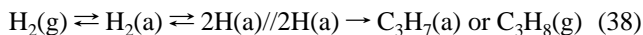


Figure 6. FR data on $\Delta I_H(t)/\Delta P_H(t)$ [mA/Torr] of a $\text{H}_2(20\text{Torr})/\text{Pt}/\text{Rh}/\text{C}_3^{2-}(20\text{Torr})$ system: (○) actual data; (■) simulated results by $J_X^*(\omega)$, of which parameters are given in Table 2. The number corresponds to the angular frequency $\omega/\text{radians min}^{-1}$: -1 ($\omega = 0.117$), 0 (=0.20), 1 (=0.89), 2 (=1.86), 3 (=2.51), 4 (=4.37), 5 (=7.41), 6 (=14.45), 7 (=44.7), 8 (=60.3), 9 (=79.4), 10 (=120). The dotted curve represents the most fitted one by $K_H^*(\omega)$.

$$\Delta I_E = \Delta(S_{+\text{IIE}} - S_{-\text{IIE}}) + \Delta R_E \quad (37)$$

On the other hand, if P_H is varied, the reaction mechanism of eq 6 should be modified to



because $\text{H}(\text{a})$ is divided into two parts by the membrane ($//$). However, H^+ -flow across the membrane, ΔI_H , may be expressed as

$$\Delta I_H = \Delta(S_{+\text{IIIH}} - S_{-\text{IIIH}}) + \Delta R_H \quad (39)$$

provided that the ratio of the atomic hydrogen on both sides of $\text{H}(\text{a})//\text{H}(\text{a})$ is constant. Equation 39 is similar in form to eq 37.

Substituting eqs 21–23 into eq 37 or 39, we have

$$\Delta I_X = k_{\text{AX}}^* \Delta A_X + (-k_{-\text{BX}} + k_{\text{BX}}^*) \Delta B_X \quad (40)$$

Substituting eqs 34 and 35 into eq 40, we have the final results:

$$\Delta I_X(t) = J_X^*(\omega) \Delta P_X(t) \quad (41)$$

where

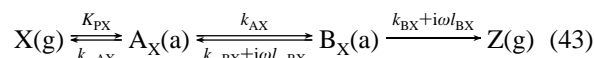
$$J_X(\omega)^* = K_{\text{PX}} k_{\text{AX}}^* (2k_{\text{BX}}^* + i\omega) / \Phi_X \quad (42)$$

Since $J_X^*(\omega)$ is characteristic of the reaction mechanism of eq 31, it may be named the characteristic function.

The seven parameters involved in $J_X^*(\omega)$ were evaluated by computer simulation on a trial and error basis. The calculated results are compared with the experimental ones of $\Delta I_X(t)/\Delta P_X(t)$ in Figures 3–6, of which parameters are summarized in Tables 1 and 2.

4. Discussion

4.1. Comparison with Previous Work. In a previous work,² a working hypothesis “only variable B is accompanied by the other variable \dot{B} ” was introduced, which leads to



This reaction mechanism is different from that of eq 31.

On the basis of eq 43, alternative characteristic functions may be derived:²

$$\Delta I_E(t) = K_C^*(\omega) \Delta P_E(t) \quad (44)$$

and

$$\Delta I_H(t) = K_H^*(\omega) \Delta P_H(t) \quad (45)$$

The results calculated from eqs 44 and 45 by the computer simulation are compared using dotted lines in Figures 3–6. Evidently, the difference between eqs 31 and 43 decreases as $\omega \rightarrow 0$ and increases with increasing ω , because both $K_C^*(\omega)$ and $K_H^*(\omega)$ are asymptotic to zero as $\omega \rightarrow \infty$, while

$$\lim_{\omega \rightarrow \infty} J_X^*(\omega) = K_{\text{PX}} l_{\text{AX}} (2l_{\text{BX}} + 1) / \{ (l_{\text{AX}} + 1)(l_{\text{BX}} + 1) \} \quad (46)$$

It is worth noting that if $l_{\text{AX}} = 0$ or $l_{\text{BX}} = -1/2$ is satisfied, $J_X^*(\omega)$ is able to be asymptotic to zero as $\omega \rightarrow \infty$. Therefore, $J_X^*(\omega)$ is more flexible than $K_C^*(\omega)$ and $K_H^*(\omega)$ so that $J_X^*(\omega)$ was superior to $K_C^*(\omega)$ and $K_H^*(\omega)$ in the curve fittings for a lot of spectra we have obtained in various separate runs.⁴ It should be emphasized that $J_X^*(\omega)$ does not require a hypothesis but is based on the novel kinetic model demonstrated in Figure 1.

The system of $\text{H}_2/\text{Rh}/\text{Rh}/\text{C}_3^{2-}$ has been investigated previously.² In the present work shown in Figures 5 and 6, the range of ω scanned was expanded in order to confirm the ability of $J_X^*(\omega)$: in the case of Figure 5, from ($\omega/\text{radians min}^{-1}$) 0.83–100 (in the previous work) to 0.12–158; in the case of Figure 6, from 5.4–56 (in the previous work) to 0.1–160. The agreement between the experimental and calculated results is considerable over the whole range of ω .

4.2. Novel Rate Constant l . The novel rate constant l 's are defined in eqs 21 and 23 as

$$l_{\text{AX}} \equiv (\partial S_{+\text{IIX}} / \partial \dot{A}_X) \quad \text{and} \quad l_{\text{BX}} \equiv (\partial R_X / \partial \dot{B}_X) \quad (47)$$

If both l 's are ignored in the mechanism of eq 31 or 43, it agrees with an ordinary one so that k_{AX}^* and k_{BX}^* contained in eqs 32 and 33 should be replaced by k_{AX} and k_{BX} ; then one finds ordinary rate equations. However, l 's were indispensable in the data analysis; the results in Tables 1 and 2 show that l 's concerned with ΔP_E are negative, but those concerned with ΔP_H are positive.

TABLE 1: Rate Constants for the System of H₂(20Torr^a)/Pt/Rh/C₃²⁻(20Torr)

| | K_{PX} (mA Torr ⁻¹) | k_{-AX} (min ⁻¹) | k_{AX} (min ⁻¹) | l_{AX} | k_{-BX} (min ⁻¹) | k_{BX} (min ⁻¹) | l_{BX} | Dev ^b (%) |
|--------------|--------------------------------------|-----------------------------------|----------------------------------|----------|-----------------------------------|----------------------------------|----------|-------------------------|
| ΔP_E | 0.124 | 2.64 | -0.197 | -0.454 | 7.50 | 1.02 | -0.490 | 3.67 |
| ΔP_H | 0.348 | 50.9 | 4.60 | 0.0183 | 2.52 | 0.336 | 0.495 | 2.22 |

^a 1 Torr = 133.32 Pa. ^b Dev = (1/N)Σ_N[(ΔI_X/ΔP_X) - J_X^{*}(ω)]² / (ΔI_X/ΔP_X)_{max}, where N denotes the number of data and (ΔI_X/ΔP_X)_{max} is the maximum value obtained in each run.

TABLE 2: Rate Constants for the System of H₂(20Torr)/Rh/Rh/C₃²⁻(20Torr)

| | K_{PX} (mA Torr ⁻¹) | k_{-AX} (min ⁻¹) | k_{AX} (min ⁻¹) | l_{AX} | k_{-BX} (min ⁻¹) | k_{BX} (min ⁻¹) | l_{BX} | Dev (%) |
|--------------|--------------------------------------|-----------------------------------|----------------------------------|----------|-----------------------------------|----------------------------------|----------|------------|
| ΔP_E | 0.0498 | 0.901 | 0.0213 | -0.612 | 5.11 | 1.3 | -0.491 | 3.72 |
| ΔP_H | 0.0554 | 8.5 | 1.14 | 0.0041 | 0.148 | 0.105 | 0.736 | 1.99 |

Numerous investigators have employed steady-state kinetic measurements in catalytic hydrogenation of light olefins. It is concluded that when the appearance rate of alkanes, R_0 , is expressed by

$$R_0 = kP_H^m P_E^n \quad (48)$$

the orders of reaction, m and n , are⁵⁻⁷

$$m \neq 1 \quad \text{and} \quad n \neq 0 \quad \text{or} \quad < 0 \quad (49)$$

Comparison with eq 47 suggests that (i) if l_X is positive, the reactant X would play an active role in the reaction, but (ii) if l_X is negative, it would play a passive role.

According to eqs 29 and 30, the relative amplitude of the free energy variation, $\Delta w/\bar{w}$, depends on l as well as μ 's. Therefore, negative or positive values of l 's suggest a nonlinear coupling of the parallel flows of free energy in the reaction mechanisms of eqs 5 and 6. On the other hand, the values of $\Delta w/\bar{w}$ depend on $\Delta\dot{A}$ or $\Delta\dot{B}$, too. When surface diffusion occurs, $\Delta\dot{A}$ or $\Delta\dot{B}$ is expected to produce heterogeneous surface concentrations because of Fick's second law:

$$\partial c/\partial t = D\nabla^2 c \quad (50)$$

It seems of interest that concentration waves of adsorbed species propagating from active zones⁸ and pattern formation of adsorbate concentrations on surfaces during heterogeneously catalyzed reactions⁹ have been observed by Ertl and co-workers.

5. Concluding Remarks

Although all rate constants of the reaction model of eq 31 have been found, the basic equations of eqs 7 and 8 contain not only the seven kinetic constants but also μ 's. Since μ_A and μ_B depend on catalysts, the kinetic parameters are not enough to predict the activity of catalysts. It would be a reason that controlling catalysts is difficult.

Since the novel rate constants, l_{AX} and l_{BX} , stem from w_A and w_B in Figure 1, the theoretical procedure in section 2 may be extended easily to another reaction model: the rate constant k of an intermediate for the direct reaction at an elementary step should be replaced by k^* ($=k + i\omega l$) in the data analysis for a reaction-rate spectrum.

It is worth noting that no l 's have been required in the data analysis for a rate spectrum obtained in a reversible or nonreactive process because of the lack of free energy dissipation.

Appendix

Substituting eqs 21 and 22 into eq 17, we have

$$\bar{A}\Delta w_A = \mu_I \Delta\dot{A} + (\mu_I - \mu_{II})\{k_A \Delta A + l_A \Delta\dot{A} - k_{-B} \Delta B - (\bar{R}/\bar{A})\Delta A\} \quad (A1)$$

As a first approximation, we may have

$$\bar{S}_{+II} = k_A \bar{A} \quad \text{and} \quad \bar{S}_{-II} = k_{-B} \bar{B} \quad (A2)$$

which are rewritten as

$$k_A = \bar{S}_{+II}/\bar{A} \quad \text{and} \quad k_{-B} = \bar{S}_{-II}/\bar{B} \quad (A3)$$

Substituting eqs A3 into eq A1, we have

$$\bar{A}\Delta w_A = \{\mu_I + l_A(\mu_I - \mu_{II})\}\Delta\dot{A} + (\mu_I - \mu_{II})\bar{S}_{-II}\{(\Delta A/\bar{A}) - (\Delta B/\bar{B})\} \quad (A4)$$

where the relation of eq 9 has been used.

Since the value of the second term on the right-hand side of eq A4 is on the order of Δ^2 , we may have

$$\bar{A}\Delta w_A = \{\mu_I + l_A(\mu_I - \mu_{II})\}\Delta\dot{A} \quad (A5)$$

On the other hand, substituting eq 23 into eq 18, we have

$$\bar{B}\Delta w_B = \{\mu_{II} + l_B(\mu_{II} - \mu_{III})\}\Delta\dot{B} + (\mu_{II} - \mu_{III})\{k_B - (\bar{R}/\bar{B})\}\Delta B \quad (A6)$$

As a first approximation, we may have

$$\bar{R} = k_B \bar{B} \quad \text{or} \quad k_B = \bar{R}/\bar{B} \quad (A7)$$

Substituting eq A7 into eq A6, we have

$$\bar{B}\Delta w_B = \{\mu_{II} + l_B(\mu_{II} - \mu_{III})\}\Delta\dot{B} \quad (A8)$$

The final results of eqs A5 and A8 seem to be reasonable, because Δw_A and Δw_B must be asymptotic to zero as $\omega \rightarrow 0$.

References and Notes

- (1) Yasuda, Y. *Heterogen. Chem. Rev.* **1994**, *1*, 103.
- (2) Yasuda, Y.; Iwai, K.; Takakura, K. *J. Phys. Chem.* **1995**, *99*, 17852.
- (3) Rekoske, J. E.; Cortright, R. D.; Goddard, S. A.; Sharma, S. B.; Dumesic, J. A. *J. Phys. Chem.* **1992**, *96*, 1880.
- (4) To be published.
- (5) Bond, G. C. *Catalysis by Metals*; Academic Press: London, 1962.
- (6) Horiuti, J.; Miyahara, K. *Hydrogenation of Ethylene on Metallic Catalysts*; NBS-NSRDS No. 13; Government Printing Office: Washington, DC, 1968.
- (7) Mann, R. S.; Lien, T. R. *J. Catal.* **1969**, *15*, 1.
- (8) Cox, M. P.; Ertl, G.; Imbihl, R. *Phys. Rev. Lett.* **1985**, *54*, 1725.
- (9) Rotermund, H. H. *Surf. Sci.* **1997**, *386*, 10.